ARTICLE
Journal of Cellular Biochemistry 107:316–327 (2009)

Journal of Cellular Biochemistry

Involvement of p53 in Phthalate Effects on Mouse and Rat Osteoblasts

M.G. Sabbieti,[1] D. Agas,[1] G. Santoni,[2] S. Materazzi,[3] G. Menghi,[1] and L. Marchetti[1*]

[1]*Department of Comparative Morphology and Biochemistry, Università di Camerino, Via Gentile III da Varano, 10 Camerino (MC), Italy*

[2]*Department of Experimental Medicine and Public Health, University of Camerino, I-62032 Camerino (MC), Italy*

[3]*Department of Chemistry, University "La Sapienza," Piazzale Aldo Moro, 10 Rome, Italy*

ABSTRACT

The role of two estrogen-mimicking compounds in regulating osteoblast activities were examined. Previously, our attention was focused on benzyl butyl phthalate (BBP) and di-*n*-butyl phthalate (DBP) since previous works showed that they enter the cytoplasm, bioaccumulate, modify actin cytoarchitecture and exert mitogenic effects involving microfilament disruption, and nuclear actin and lamin A regulation in Py1a rat osteoblasts. In this study we showed that BBP and DBP cause DNA base lesions both in MT3T3-E1 osteoblasts and in mouse primary calvarial osteoblasts (COBs). In addition, treatment with the above effectors caused an increase of p53 and phospho-p53 (ser-15 and ser-20) as well as an increase of apoptotic proteins with consequent decrease of cell viability. Moreover, treatment with phthalates did not modified p53 and phospho-p53 expression in Py1a rat osteoblasts. It is of relevance that in p53 knockdown mouse osteoblasts a proliferative effect of phthalates, similar to that observed in rat Py1a osteoblasts, was found. In conclusion, our data demonstrated that phthalates induce osteoblast apoptosis, which is, at least in part, mediated by p53 activation, suggesting that the proliferative effects could be due to p53 missing activation or p53 mutation. J. Cell. Biochem. 107: 316–327, 2009.

KEY WORDS: APOPTOSIS; p53; PHTHALATES; SIRNA; BONE

DNA-damaging agents lead to the activation of specific checkpoints. One of the key proteins in these pathways is the tumor suppressor p53 [Dewey et al., 1995; Ross, 1999]. p53 exerts its function mainly through transactivational activity, including the induction of CDKN1/p21, 14-3-3δ and Reprimo for G_1–G_2 arrest [Bunz et al., 1998; Ohki et al., 2000], p53R2 for DNA repair [Tanaka et al., 2000] and Bax, Puma and p53AIP1 for apoptosis [Attardi et al., 2000]. It is known that p53 activates cell cycle arrest and DNA repair or apoptosis after DNA damage depending on the extent of unrepaired or misrepaired double-strand breaks in the DNA [Offer et al., 2002; Fei and El-Deiry, 2003]. Both cell cycle arrest or apoptosis appear to be involved in p53 ability to suppress tumorigenesis. Another important protein involved in the response to DNA damage is the ATM protein kinase that interacts with p53 causing phosphorylation at ser 15 [Savitsky et al., 1995; Morgan and Kastan, 1997; Siliciano et al., 1997; Banin et al., 1998].

It is known that bone remodeling is controlled by various hormones and cytokines [Rodan, 1992]. An imbalance between bone formation and bone resorption leads to metabolic bone diseases [Parfitt, 1987]. Since estrogens deficiency is also liable for important bone diseases, as osteoporosis, the role of estrogens as well as estrogen-mimicking compounds, like phthalates, in regulating activities of bone cells is crucial to understand some bone metabolism pathologies. In particular, phthalate esters were selected as they are global contaminants, characterized by a variety of industrial uses, widely distributed in the environment, and often occurring at low levels in food [Group, 1986; Sharman et al., 1994]. Their toxic potential was referred to many years ago [Mayer et al., 1972] and it has been found that they can also be regarded as endocrine disruptors (EDs) with estrogenic activity [Jobling et al., 1995; Harris et al., 1997]. It has been demonstrated that benzyl butyl phthalate (BBP) and di-*n*-butyl phthalate (DBP) have potential

M.G. Sabbieti and D. Agas contributed equally to this work.

Grant sponsor: The Italian Ministry of University and Research (PRIN 2005); Grant sponsor: University of Camerino, Fondazione Carima, Italy.

*Correspondence to: Prof. L. Marchetti, Department of Comparative Morphology and Biochemistry, University of Camerino, I-62032 Camerino (MC), Italy. E-mail: luigi.marchetti@unicam.it

Received 4 August 2008; Accepted 10 February 2009 • DOI 10.1002/jcb.22127 • 2009 Wiley-Liss, Inc.

Published online 27 March 2009 in Wiley InterScience (www.interscience.wiley.com).

activity as EDs. Indeed, EDs exert their action by binding to the estrogen receptor and regulating the activity of estrogen responsive genes [Jobling et al., 1995; Guillette et al., 1996; Harris et al., 1997; Longnecker et al., 1997; Safe, 1998]. Some of them have been also found to cause a significant increase in the number of skeletal malformations [Ema et al., 1993].

Previously, it has been demonstrated that BBP and DBP enter the cytoplasm of Py1a rat osteoblasts inducing both bioaccumulation and nuclear translocation of FGF-2 [Sabbieti et al., 2000; Menghi et al., 2001]. Additional studies indicated that the actin cytoskeleton of Py1a rat osteoblasts undergoes modifications upon phthalate administration and that BBP and DBP exert their action in a similar way; indeed, they act rapidly, transiently and in a dose- and time-related manner on osteoblast morphology disrupting the cytoplasmic and the nuclear actin organization as well as lamin A [Marchetti et al., 2002; Agas et al., 2007].

In the present study we aimed to demonstrate the short term and long-term effects of BBP or DBP on mouse osteoblasts; in particular, our attention was focused on phospho-ATM and phospho-p53 expression as well as on the apoptotic pathways. The effects exerted by phthalates were also investigated by p53 silencement.

MATERIALS AND METHODS

In order to study the effects exerted by BBP or DBP, MC3T3-E1 mouse osteoblasts were utilized. MC3T3-E1 cells are non-transforming cell line derived from newborn mouse calvariae displaying osteoblast-like characteristics. They also undergo a normal developmental sequence of osteoblast differentiation in association with the expression of bone markers [Quarles et al., 1992; Stein and Lian, 1993]. Some critical experiments were also performed on mouse primary calvarial osteoblasts (COBs) and on Py1a rat osteoblasts.

EXPERIMENTAL ANIMALS

Harlan Sprague–Dawley ICR (CD-1) male mice (Harlan, Italy) were used. Mice were sacrificed by CO_2 narcosis and cervical dislocation in accordance with the recommendation of the Italian Ethical Committee and under the supervision of authorized investigators.

PRIMARY CALVARIAL OSTEOBLASTS (COBS)

COBs were obtained from newborn mice by sequential digestion with 0.1% collagenase (Roche Diagnostic, Milano, Italy), as previously described [Montero et al., 2000]. Cells were pooled and then cultured to confluence in 100-mm dishes.

Assessment of DNA damage. MC3T3-E1 osteoblasts and COBs were plated at 15,000 cells/cm^2 in 6-well culture dishes (Costar Corp., Celbio, Italy) in Dulbecco's Modified Eagle's Medium (DMEM; Sigma–Aldrich S.r.l., Milano, Italy) with 10% heat inactivated fetal calf serum (FCS; Invitrogen, Milano, Italy), penicillin and streptomycin. Cells were grown for 4 days to ~80% confluence. Cells were pre-cultured for another 24 h in serum-free DMEM with antibiotics before treatment with BBP (10^{-6} M) or DBP (10^{-6} M) (Sigma–Aldrich S.r.l.) for additional 24 h. Control cultures were pulsed with only vehicle. The genomic DNA isolation was performed using Genomic DNA isolation kit (BioVision, Vinci-Biochem, Firenze, Italy) according to the manufacturer's instructions.

Finally, the DNA concentration was adjusted (0.1 μg/μl) as required from the DNA damage quantification kit (BioVision, Vinci-Biochem) that was used to determine the level of apurinic/apyrimidinic (AP) sites. Since it has been estimated that about 2×10^5 base lesions are generated per cell per day, the level of AP sites in cells is an indicator of DNA lesion.

Cell cultures for Western blotting. Mouse MC3T3-E1 osteoblasts and rat Py1a osteoblasts were plated at 15,000 cells/cm^2 in 6-well culture dishes (Costar Corp.) in DMEM (Sigma–Aldrich S.r.l.), supplemented with 10% heat inactivated FCS (Invitrogen), penicillin and streptomycin, for only mouse osteoblast, or in F-12 culture medium with 5% non-heat inactivated FCS, penicillin and streptomycin, for only rat osteoblasts. Cells were grown for 5–6 days to confluence, then cultures were serum deprived for 24 h and treated with BBP or DBP (from 10^{-5} to 10^{-8} M), or vehicle for selected time periods.

PROTEIN LEVELS

Proteins were extracted with Cytobuster Protein extraction reagent (Inalco SPA, Milano, Italy) and concentration was determined by the BCA protein assay reagent (Pierce, Rockford, Celbio, Milano Italy). After SDS–polyacrylamide gel electrophoresis (PAGE) on 12% gels, proteins were transferred to PVDF membranes (Amersham Biosciences, Europe, GMBH). The next steps were performed by ECL Advance Western Blotting Detection Kit (Amersham Biosciences, GMBH). Briefly, membranes were blocked with Advance Western Blotting Agent (Amersham Biosciences, GMBH) in PBS-T (PBS containing 0.1% Tween-20) for 1 h at room temperature. Then, membranes were incubated with the following antibodies: mouse anti-phospho-ATM antibody, (Cell Signaling, Celbio, Italy) diluted 1:500; rabbit anti-p53, rabbit anti-phospho-p53 specifically phosphorylated at ser-15 and ser-20 antibodies, (Cell Signaling) all diluted 1:500; rabbit anti-cytochrome *c*, anti-Apaf-1, anti-cleaved caspase-9, anti-cleaved caspase-3, anti-cyclin D3, anti-CDK4 antibodies (Cell Signaling), all diluted 1:500; rabbit anti-Bax, anti-p21 antibodies (Santa Cruz Biotechnology, Inc., Italy), all diluted 1:200; mouse anti-c-myc antibody (Santa Cruz Biotechnology, Inc.) diluted 1:200. All membranes were incubated with the above primary antibodies for 2 h at room temperature. After washing with PBS-T the blots were incubated with horseradish peroxidase (HRP)-conjugated rabbit anti-mouse IgG antibody (Amersham Biosciences, GMBH) or with HRP-conjugated donkey anti-rabbit IgG antibody (Amersham Biosciences, GMBH) both diluted 1:100,000 in blocking solution for 1 h at room temperature. After further washing with PBS-T, immunoreactive bands were visualized using luminol reagents and Hyperfilm-ECL film (Amersham Biosciences, GMBH) in accordance with the manufacturer's instructions. To normalize the bands, filters were stripped and re-probed with mouse anti-α-tubulin antibody (Sigma–Aldrich). Band densities were quantified densitometrically.

SUBCELLULAR FRACTIONATION

MC3T3-E1 osteoblasts were plated in 6-well culture dishes (Costar Corp.) at the density of 15,000 cells/cm^2 and grown for 6 days in DMEM medium with 10% heat inactivated FCS, penicillin and streptomycin. Then, cells were pre-cultured for another 24 h in serum-free DMEM with antibiotics, before addition of BBP (10^{-6} M), or vehicle for 30 min, 2 h, 6 h or 24 h. Cellular fractionation was performed with a Qproteome Cell Compartment Handbook (Qiagen SPA, Milano, Italy) in accordance with the manufacturer's instructions. Then, fractions were processed as above described and filters were incubated with the rabbit anti-Bax, anti-phospho-Rb (ser-780), and anti-total-Rb antibodies (Santa Cruz Biotechnology, Inc.) all diluted 1:200 for 2 h and the rabbit anti-cytochrome *c* (Cell Signaling) diluted 1:500 for 2 h at room temperature. The next steps were performed as above described. To normalize the bands, filters were stripped and re-probed with mouse anti-α-tubulin (Sigma–Aldrich), mouse anti-YY1 (Santa Cruz Biotechnology, Inc.) and rabbit anti-VDAC (Cell Signaling) antibodies. Band densities were quantified densitometrically.

Assessment of the metabolic activity of viable cells (MTS). The metabolic activity of viable cells was determined by the MTS [3-(4,5-dimethylthiazol-2-yl)-5-(3-carboxymethoxyphenyl)-2-(4-sulfophenyl)-2H-tetrazolium] assay. Briefly, MC3T3-E1 cells and COBs were plated at the density of 5,000 cells/well in 96-well culture dishes (Costar Corp.) and grown in DMEM medium supplemented with 10% heat inactivated FCS, penicillin and streptomycin to ~80% confluence. Cells were serum deprived for 24 h and treated with BBP (10^{-6} M), DBP (10^{-6} M), or vehicle for additional 24 h. Subsequently, cells were incubated with 20 μl/well of CellTiter 96 AQ_{ueous} One Solution Reagent (Promega Italia S.r.l., Milano, Italy) and incubated for 2 h in a humidified, 5% CO_2 atmosphere. The quantity of formazan product is directly proportional to the number of living cells in culture. The colored formazan was measured by reading the absorbance at 490 nm using a 96-well plate reader.

STATISTICAL ANALYSIS

The significance of difference between two groups was evaluated with an unpaired two-tailed Student's *t*-test.

Cell cycle analysis. 3×10^5/ml MC3T3-E1 cells were grown with BBP (10^{-6} M) or vehicle for 24 h at 37°C and 5% CO_2. After washing in PBS, cells were fixed for 30 min on ice by adding 1 ml of 70% cold ethanol, centrifuged in order to discard ethanol, stained for 45 min at room temperature with Propidium Iodide (PI) 20 μg/ml in DNAse-free PBS, and finally analyzed by flow cytometry. The percentage of positive cells determined over 10,000 events was analyzed on a FACScan cytofluorimeter using the CellQuest software (Becton Dickinson). Fluorescent intensity is expressed in arbitrary units on a logarithmic scale.

Fluorescein-FragEL™ DNA fragmentation detection method. The Fluorescein-FragEL™ Kit (Calbiochem, Milano, Italy) is a method for the labeling of DNA breaks in apoptotic nuclei in cell preparations fixed on coverslips. Briefly, MC3T3-E1 osteoblasts and COBs were plated at 3,500 cells/cm^2 in 6-well culture dishes containing coverslips, previously cleaned and sterilized, in DMEM medium supplemented with 10% heat inactivated FCS, penicillin and streptomycin. Cells were grown for 4 days to ~80% confluence. Then, cells were serum deprived for 24 h before treatment with BBP (10^{-6} M), DBP (10^{-6} M), or vehicle for additional 24, 48, and 72 h. After administration of the effectors, cells were briefly rinsed with PBS 0.1 M, pH 7.4, and fixed in 4% paraformaldehyde (PFA), diluted in PBS for 25 min at room temperature. Then, they were dehydrated in 80% ethanol and rehydrated in 1× Tris buffered saline (TBS) solution for 15 min at room temperature. Cells were permeabilized with 2 mg/ml Proteinase K diluted 1:100 in 10 mM Tris, pH 8, for 5 min at room temperature. Then, samples were covered with 100 μl of 1× terminal deoxyribonucleotidyl transferase (TdT) equilibration buffer for 30 min at room temperature. After removal of the equilibration buffer, each coverslip was covered with 60 μl of TdT labeling reaction mixture prepared with 57 μl Fluorescein-FragEL™ TdT Labeling reaction mix and 3 μl TdT enzyme for 90 min at 37°C. Finally, coverslips were mounted on slides using Fluorescein-FragEL™ Mounting Media. The quantitative analysis was performed by direct counting in the Zeiss Axiophot. Using the 20× objective lens, the number of apoptotic cells was counted in 30 areas (15 cells/area) for each slide as previously performed for TUNEL method [Hecht et al., 2000].

Phospho-p53 immunolabeling at confocal laser scanning microscopy (CLSM) level. MC3T3-E1 mouse osteoblasts and Py1a rat osteoblasts were plated at 3,500 cells/cm^2 in 6-well culture dishes containing coverslips, previously cleaned and sterilized, in DMEM (Sigma–Aldrich S.r.l.), supplemented with 10% heat inactivated FCS, penicillin and streptomycin, for only mouse osteoblasts, or in F-12 culture medium with 5% non-heat inactivated FCS (Invitrogen) penicillin and streptomycin, for only rat osteoblasts. Cells were grown for 4 days to ~80% confluence. Then, cells were pre-cultured for another 24 h in serum-free culture medium before treatment with BBP (10^{-6} M), DBP (10^{-6} M), or vehicle for additional 6 h. After administration of the effectors, cells were briefly rinsed with PBS 0.1 M, pH 7.4, and fixed in 4% PFA, diluted in PBS for 25 min at room temperature. Cells were washed three times in PBS, permeabilized with 0.3% Triton X-100 for 30 min, and incubated with 0.5% BSA diluted in PBS for 20 min at room temperature. Cells were incubated with a 1:50 dilution of the rabbit anti-phospho-p53 (ser-15) antibody (Cell Signaling) in PBS for 2 h at room temperature. After rinsing, cells were incubated with a 1:75 dilution of goat anti-rabbit IgG conjugated with fluorescein isothiocyanate (FITC; Sigma–Aldrich) in PBS for 90 min at room temperature.

Control experiments were performed by omitting the primary antibody. After a washing step, coverslips were mounted on slides with PBS/glycerol (1:1).

CONFOCAL ANALYSIS AND IMAGE ACQUISITION

Immunofluorescence patterns were analyzed under a Bio-Rad Ar/Kr MRC-600 Confocal Laser Scanning Microscopy (Bio-Rad, Herdfordshire, UK) attached to a Nikon Diaphot-TMD-EF inverted microscope equipped with a Plan Apo, oil immersion, objective (×60, NA = 1.4) to obtain optical sectioning of samples [Shotton, 1989; Pawley, 1995]. The standard BHS block (excitor filter 488 DF 10) was used for

FITC signals. High-resolution images for a qualitative evaluation of the immunofluorescence patterns were captured and analyzed with Confocal Assistant 4.02 (Bio-Rad) and finally transferred to PhotoShop v7.0 (Adobe) for generation of graphics.

RNA interference (RNAi). MC3T3-E1 osteoblasts were transfected with p53 siRNA according to siRNA transfection protocol from manufacture (Santa Cruz Biotechnology, Inc.). A control siRNA (non-homologous to any known gene sequence) was used as a negative control. The levels of p53 were analyzed by Western blotting using the rabbit anti-p53 antibody (Cell Signaling) and the specificity of the silencing was confirmed in three different experiments. Osteoblasts transfected with control siRNA and with p53 siRNA were 24 h serum deprived before addition of BBP (10^{-6} M), DBP (10^{-6} M), or vehicle for 6 and 24 h. Then, proteins were extracted and Bax, cleaved caspase 9 as well as cyclin D3 levels were analyzed by Western blotting as described above. To normalize the bands, filters were stripped and re-probed with the monoclonal anti-α-tubulin antibody. Band densities were quantified densitometrically.

Assessment of the metabolic activity of viable cells (MTS) on p53 silenced MC3T3-E1 osteoblasts. Osteoblasts transfected with control siRNA and with p53 siRNA were 24 h serum deprived before addition of BBP (10^{-6} M), DBP (10^{-6} M), or vehicle for additional 24 h. The next steps were performed as above described.

Cell cultures for immuno electron microscopy (IEM). Py1a and MC3T3-E1 osteoblasts were prepared as previously reported [Marchetti et al., 2006]. Briefly, they were plated at 5,000 cells/cm^2 on 100 mm culture dishes and grown for 5 days in DMEM (Sigma–Aldrich S.r.l.), supplemented with 10% heat inactivated FCS (Invitrogen), penicillin and streptomycin, for only mouse osteoblast, or in F-12 culture medium with 5% non-heat inactivated FCS, penicillin and streptomycin, for only rat osteoblasts. After 80% confluence, cells were pre-cultured in serum-free F-12 containing antibiotics and 1 mg/ml BSA for another 24 h. Then, cells were treated with BBP (10^{-6} M) for additional 6 h. Control cultures were only pulsed with vehicle. After rinsing twice in the appropriate medium and one quick washing in 0.1 M cacodylate buffer, pH 7.4, cells were fixed on plates with 4% PFA and 0.5% glutaraldehyde in 0.1 M cacodylate buffer, pH 7.4, for 3 h at 4°C. Then, cells were rinsed several times for 30 min in 0.1 M PBS, pH 7.3, containing 0.1% BSA and 7% sucrose, at 4°C. Finally, cells collected in Falcon tubes, centrifuged and pre-embedded in agarose were dehydrated in methanol from 50% to 90%, and embedded in Unicryl resin (BBInternational Ltd., Cardiff, UK) for 72 h at 4°C under U.V. lamp. Ultra-thin sections (about 60 nm thick) from plastic embedding were cut by means of an LKB Ultrotome V and collected on uncoated 400 mesh nickel grids.

Floating ultra-thin sections were rehydrated with 0.05 M TBS solution, pH 7.6, and pre-incubated with 1% BSA, fatty acid free, in TBS, pH 7.6, for 30 min at room temperature. Grids were then incubated with 1:40 dilution of the rabbit anti-phospho-p53 (ser-15) antibody (Cell Signaling) in TBS for 2 h at room temperature, in a humid chamber. After rinsing, the signals were developed with 1:10 dilution of the goat anti-rabbit IgG (40 nm gold labeled IgG) (Sigma–Aldrich S.r.l.), in TBS, pH 7.6, containing 0.05% Tween-20 for 90 min at room temperature, in a humid chamber. Sections were then washed several times in TBS, pH 7.6, and in distilled water. All sections were finally counterstained with uranyl acetate (5 min) and lead citrate (2 min) at room temperature. Control experiments were carried out by omitting the appropriate primary antibody. All specimens were analyzed by means of a Philips EM 201C electron microscope at an accelerating voltage of 60 kV.

Image analysis for phospho-p53 (ser-15) was performed on Scion Image Beta 4.03 for Windows XP and gold particle counts were done on micrographs at a final magnification of 35,000×. Immunogold labeling density (gold particles/μm^2) of vehicle and treated osteoblasts were compared using a *t*-test.

RESULTS

EFFECTS OF PHTHALATES ON DNA DAMAGE

The effects of BBP or DBP on the DNA base lesions in MC3T3-E1 osteoblasts and COBs were examined. In particular, 24 h of treatment with the above effectors provoked a generation of 33×10^5 base lesions per cell in MC3T3-E1 cells; similar results were obtained in COBs (Fig. 1A). Since DNA damaging agents activate p53 by a family of protein kinases including ATM, we investigated the roles of the tested phthalates on phospho-ATM (ser-1981), p53 and phospho-p53 (ser-15 and ser-20) expressions. Indeed, Western blotting experiments showed that phospho-ATM levels were increased after 6 and 24 h of 10^{-6} M BBP treatment (Fig. 1B). Since overlapping results were also found by using 10^{-5} M BBP for 6 h as shown in dose–response studies (Fig. 1C), all the following assays were performed at concentration of 10^{-6} M. The lowest effective concentration was chosen to minimize the cell toxicity based on our previous studies [Agas et al., 2007]. Moreover, an increase of p53, phospho-p53 (ser-15) and phospho-p53 (ser-20) was found after 6 and 24 h of BBP treatment (Fig. 1D). Consistently, treatment with BBP for 6 h caused an increased expression of the cyclin-dependent kinase inhibitor p21, a downstream transcriptional target of p53 (Fig. 1E). Overlapping results were also obtained after DBP treatment (data not shown). Pooled data from three different experiments better clarified that BBP or DBP exert their maximal effects at 6 h (Fig. 1F).

EFFECTS OF PHTHALATES ON APOPTOTIC PATHWAY

It is largely accepted that p53 phosphorylation induces cell cycle arrest or apoptosis through several mediators. In our experiments we firstly examined the levels of the proapoptotic protein Bax on MC3T3-E1 osteoblasts. Time-course Western blotting experiments showed that BBP increased Bax levels starting from 2 up to 24 h (Fig. 2A1). Western blotting revealed that the increase of Bax protein was particularly evident at 6 h of BBP treatment; thus subcellular fractions were examined and both nuclear and mitochondrial extracts confirmed this datum (Fig. 2A2). It has been demonstrated that translocation of Bax from the cytosol to the mitochondrial outer membrane causes a release of cytochrome *c* which interacts with protein Apaf-1 leading to the activation of pro-caspase 9 with

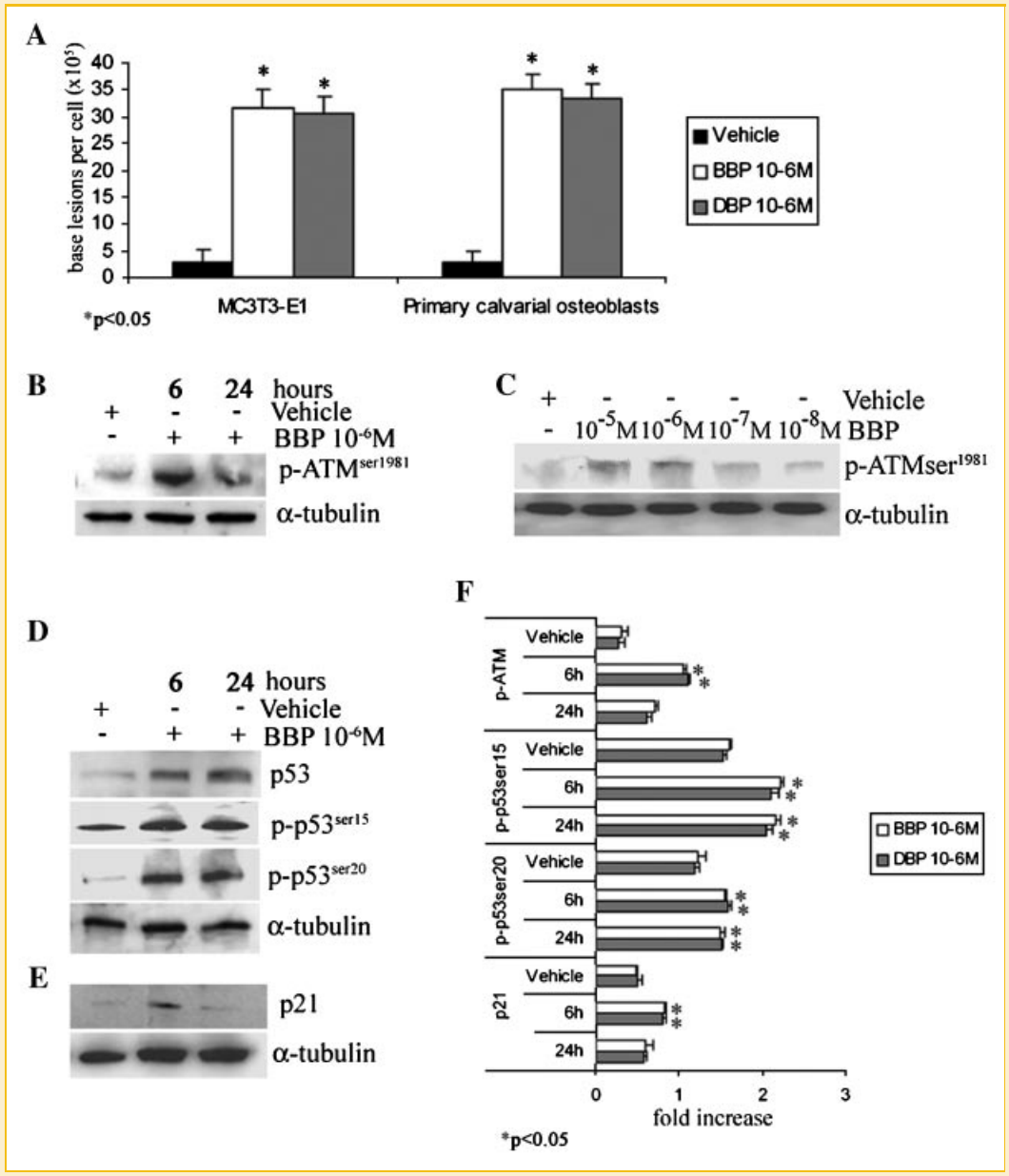

Fig. 1. A: Effects of BBP and DBP on DNA damage in MC3T3-E1 and primary calvarial osteoblasts. Values were referred as means ± standard deviation (SD) and statistically analyzed with *t*-test operating on PC computer. Note the significant increase of base lesions per cell in 24 h BBP (10^{-6} M) and DBP (10^{-6} M) treated cells compared to vehicle treated cells; $^{*}P < 0.05$. B,C: Time course-dose response effects of BBP on phospho-ATM in MC3T3-E1 osteoblasts. Phospho-ATM levels were analyzed by Western blotting as described in Materials and Methods Section. Cells were serum deprived for 24 h and treated with BBP (10^{-6} M) or vehicle for 6 and 24 h (B) or with BBP (from 10^{-5} M to 10^{-8} M), or vehicle for 6 h (C). Proteins (5 μg) from each sample were subjected to SDS–PAGE, transferred to PVDF membrane and probed with mouse anti-phospho-ATM. D,E: Effects of BBP on p53, phospho-p53 (ser-15 and ser-20), and p21 in MC3T3-E1 osteoblasts. p53, phospho-p53 (ser-15 and ser-20), and p21 levels were analyzed by Western blotting as described in Materials and Methods Section. Cells were serum deprived for 24 h and treated with BBP (10^{-6} M) or vehicle for 6 and 24 h. Proteins (5 μg) from each sample were subjected to SDS–PAGE, transferred to PVDF membrane and probed with rabbit anti-p53, rabbit anti-phospho-p53 (ser-15) rabbit anti-phospho-p53 (ser-20) (D), and rabbit anti-p21 (E) antibodies; then, filters were stripped and re-probed with mouse anti-α-tubulin antibodies to show equal amount of loading. F: Statistical analysis from a pool of three different experiments showing the effects of BBP and DBP on the above proteins. Values were referred as means ± SD and statistically analyzed with *t*-test operating on PC computer. Note the significant increase particularly after 6 h of BBP and DBP treatment, compared to vehicle treated cells; $^{*}P < 0.05$.

consequent caspase cascade; accordingly, we investigated the effects of BBP and DBP on this pathway. Western blotting experiments showed that treatment with BBP caused an increased level of cytochrome *c* starting from 30 min up to 24 h (Fig. 2B1). In particular, the increase of cytochrome *c* was maximal at 2 h in the mitochondrial fraction and at 24 h in the cytoplasmic one (Fig. 2B2). An increased Apaf-1 level was observed already from 30 min of BBP treatment (Fig. 2C). Consistently, treatment with BBP from 2 to 24 h strongly increased both cleaved caspase 9 and cleaved caspase 3 (Fig. 2D).

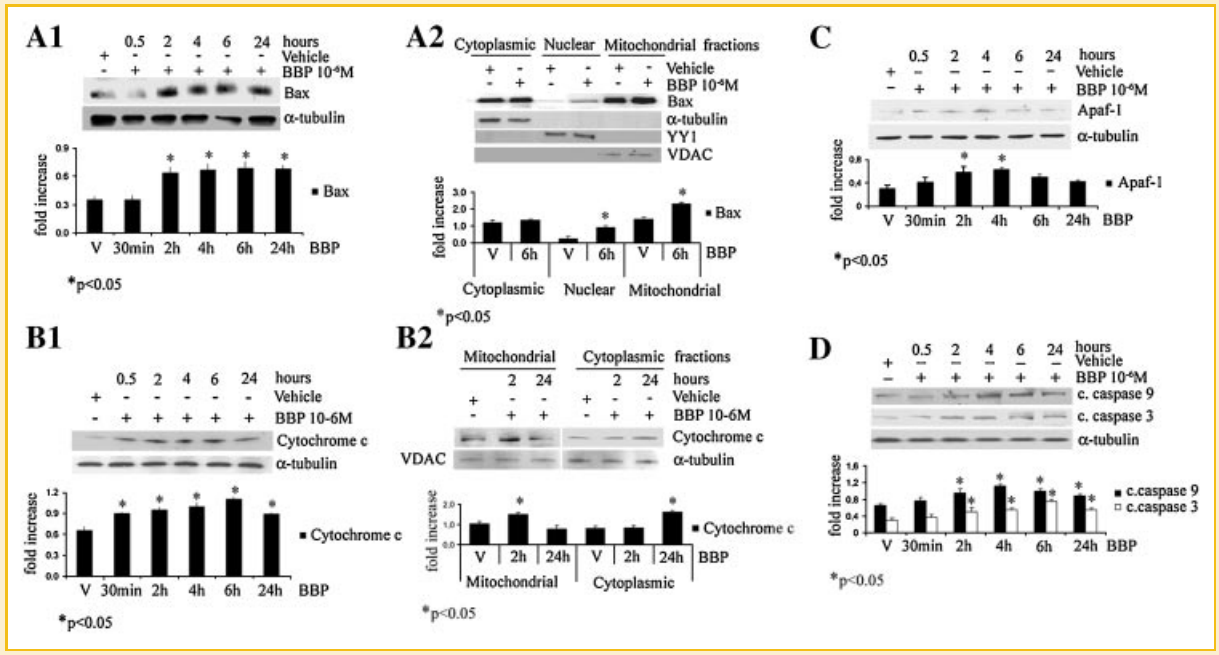

Fig. 2. A1: Time-course effects of BBP on Bax livels in MC3T3-E1 osteoblasts. Bax levels were analyzed by Western blotting as described in Materials and Methods Section. Cells were serum deprived for 24 h and treated with BBP (10^{-6} M) or vehicle for selected time periods. Proteins (5 μg) from each sample were subjected to SDS–PAGE, transferred to PVDF membrane and probed with rabbit anti-Bax antibody; then, filters were stripped and re-probed with mouse anti-α-tubulin antibody to show equal amount of loading. A2: Effects of BBP on Bax levels in cytoplasmic, nuclear, and mitochondrial fractions from MC3T3-E1 osteoblasts. Cells were serum deprived for 24 h and treated with BBP (10^{-6} M) or vehicle for 6 h. Cellular fractionations were performed with a Qproteome Cell Compartment Handbook. Proteins (5 μg) from each sample were subjected to SDS–PAGE, transferred to PVDF membrane and probed with the rabbit anti-Bax antibody. Then, filters were stripped and re-probed with mouse anti-α-tubulin, mouse anti-YY1, and rabbit anti-VDAC antibodies to show equal amount of loading. B1: Time-course effects of BBP on cytochrome *c* levels in MC3T3-E1 osteoblasts. The protein levels were analyzed by Western blotting as described in Materials and Methods Section. Cells were serum deprived for 24 h and treated with BBP (10^{-6} M) or vehicle from 30 min up to 24 h. Proteins (5 μg) from each sample were subjected to SDS–PAGE, transferred to PVDF membrane and probed with rabbit anti-cytochrome *c*; then, filters were stripped and re-probed with mouse anti-α-tubulin antibody to show equal amount of loading. B2: Effects of BBP on cytochrome *c* levels in mitochondrial and cytoplasmic fractions from MC3T3-E1 osteoblasts. Cells were serum deprived for 24 h and treated with BBP (10^{-6} M) or vehicle for 2 and 24 h. Cellular fractionations were performed with a Qproteome Cell Compartment Handbook. Proteins (5 μg) from each sample were subjected to SDS–PAGE, transferred to PVDF membrane and probed with the rabbit anti-cytochrome *c* antibody. Then, filters were stripped and re-probed with mouse anti-α-tubulin and rabbit anti-VDAC antibodies to show equal amount of loading. C,D: Time-course effects of BBP on Apaf-1, cleaved caspase 9 and cleaved caspase 3 in MC3T3-E1 osteoblasts. Cells were serum deprived for 24 h and treated with BBP (10^{-6} M) or vehicle from 30 min up to 24 h. Proteins (5 μg) from each sample were subjected to SDS–PAGE, transferred to PVDF membrane and probed with rabbit anti-Apaf-1 (C), rabbit anti-cleaved caspase 9 and rabbit anti-cleaved caspase 3 (D) antibodies; then, filters were stripped and re-probed with mouse anti-α-tubulin antibody to show equal amount of loading.

In parallel with an increase of the apoptotic proteins, the phthalate effects on the proto-oncogen protein c-myc, CDK4, and cyclin D3 were investigated. Time-course experiments showed that BBP caused a decrease of c-myc (Fig. 3A) as well as CDK4 and cyclin D3 (Fig. 3B) starting from 2 to 24 h. To verify whether the observed reduction in cyclin D1 protein might influence the endogenous Rb phosphorylation, Western blot analyses for phospho-Rb (ser-780) and total Rb were performed with nuclear extracts incubated for 6 and 24 h with BBP. BBP treatment determined a reduction of Ser-780 Rb phosphorylation, a target for specific cdk4/6-dependent phosphorylation in vitro. Total Rb protein level was constant throughout the experiment in all sample (Fig. 3C). Each experiment in Figures 2 and 3 was performed, at least three times, with overlapped results; $P < 0.05$. Similar data were obtained after DBP treatment (data not shown).

EFFECTS OF PHTHALATES ON OSTEOBLAST VIABILITY AND CELL CYCLE

MTS assay was performed to examine also the metabolic activity of viable MC3T3-E1 osteoblasts and COBs and it was found that the treatment with BBP and DBP for 24 h caused significant decrease of cell viability (Fig. 4A). Moreover, the effects of BBP on cell cycle was examined; the results obtained evidenced that treatment with BBP for 24 h generate a 96.30% of cell population in G0/G1 phase respect to the 76% found in vehicle treated cells (Fig. 4B). Furthermore, Fluorescein FragEL™ assay demonstrated a statistically significant increase of apoptotic MC3T3-E1 osteoblasts (Fig. 4C) and COBs (data not shown) after 24 h of BBP and DBP treatment.

DAILY TREATMENT OF PHTHALATES FROM 24 TO 72 H

The effects of BBP and DBP daily administration were followed for 3 days. Western blotting experiments showed that treatment with BBP from 48 to 72 h induced a clear increase of phospho-p53 (ser-15) as well as Bax and caspases 9 and 3 levels (Fig. 5A).

It was also demonstrated, by MTS assay, that treatment with BBP or DBP for 48 and 72 h caused a more consistent decrease of cell viability compared to that observed after 24 h in both MC3T3-E1 osteoblasts and COBs (Fig. 5B). In addition, phthalate administration for 72 h induced a severe increase of apoptotic cells as showed by Fluorescein FragEL™ assay (Fig. 5C).

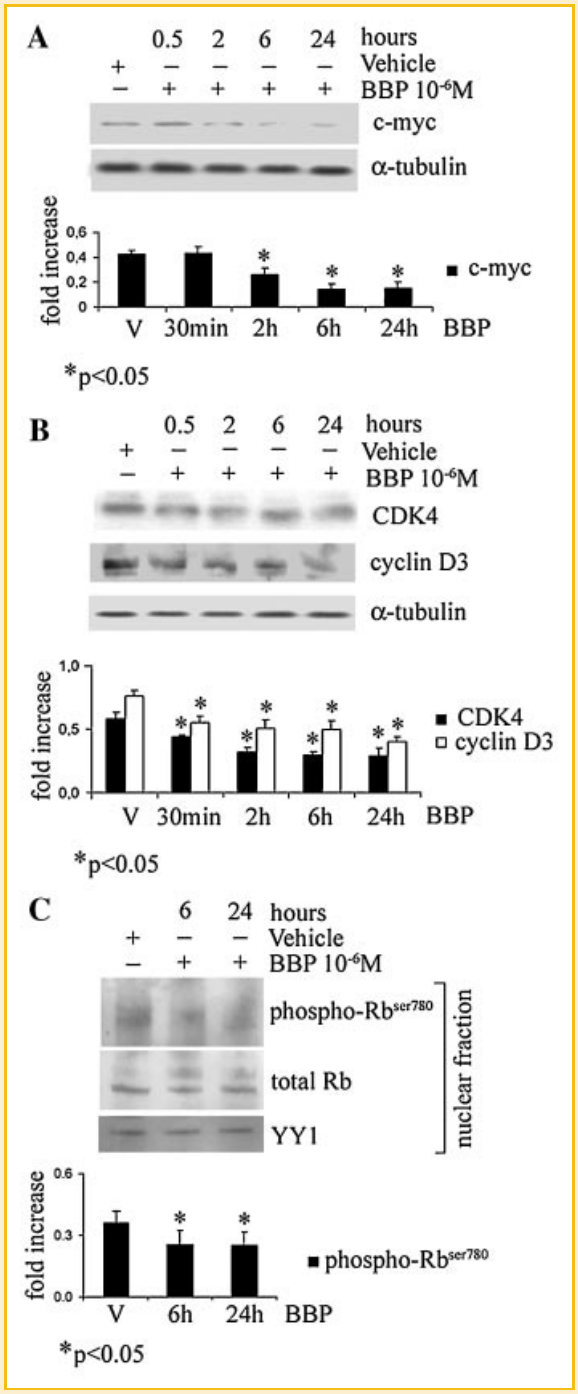

Fig. 3. A,B: Effects of BBP on c-myc, Cyclin D3, and CDK4 in MC3T3-E1 osteoblasts. Cells were serum deprived for 24 h and treated with BBP (10^{-6} M) or vehicle from 30 min up to 24 h. Proteins (5 μg) from each sample were subjected to SDS–PAGE, transferred to PVDF membrane and probed with mouse anti-c-myc (A), rabbit anti-CDK4, and mouse anti-cyclin D3 (B) antibodies; then, filters were stripped and re-probed with mouse anti-α-tubulin antibody to show equal amount of loading. C: Effects of BBP on phospho-Rb (ser-780) and total Rb levels in nuclear fraction from MC3T3-E1 osteoblasts. Cells were serum deprived for 24 h and treated with BBP (10^{-6} M) or vehicle for 6 and 24 h. Cellular fractionations were performed with a Qproteome Cell Compartment Handbook. Proteins (5 μg) from each sample were subjected to SDS–PAGE, transferred to PVDF membrane and probed with rabbit anti-phospho-Rb (Ser-780) or rabbit anti-total-Rb antibodies. Then, filters were stripped and re-probed with mouse anti-YY1 to show equal amount of loading.

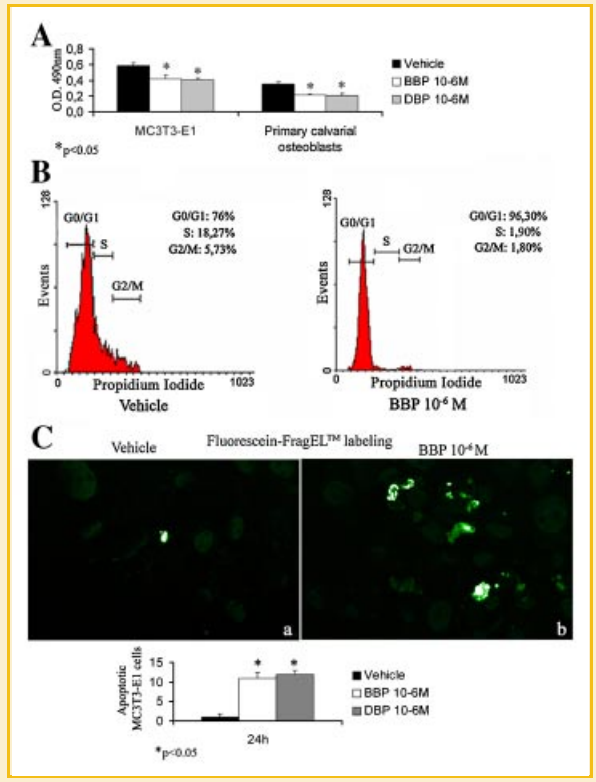

Fig. 4. A: Effects of BBP and DBP on the metabolic activity of viable MC3T3-E1 osteoblasts and COBs. Cells were serum deprived for 24 h and treated with BBP (10^{-6} M), DBP (10^{-6} M), or vehicle for additional 24 h. Values are mean ± SEM for three different experiments. Note that BBP and DBP significantly decreased cell viability in both cellular models; $^{*}P < 0.05$. B: Effects of BBP on cell cycle progression in MC3T3-E1 osteoblasts. The distribution of cell population through the cell cycle phase after BBP treatment was evaluated by flow cytometry and the percentage of cells in different phases of the cycle was calculated using the CellQuest software (Becton Dickinson). Fluorescent intensity was expressed in arbitrary units on a logarithmic scale. C: Effects of BBP and DBP on DNA fragmentation. Cells were serum deprived for 24 h and treated with BBP (10^{-6} M), DBP (10^{-6} M), or vehicle for additional 24 h. Representative photomicrographs of Fluorescein-FragEL-positive osteoblasts that increased after 24 h of BBP or DBP treatment (b) respect to vehicle treated osteoblasts (a). The quantitative analysis was performed as previously described in Materials and Methods Section. Values were referred as means ± SD and statistically analyzed with *t*-test operating on PC computer; $^{*}P < 0.05$.

Summarizing, the complex of data suggested that apoptotic effects of phthalates on mouse osteoblasts could be due to p53 activation; thus p53 silencing was performed.

EFFECTS OF PHTHALATES ON p53 SILENCED MC3T3-E1 OSTEOBLASTS

siRNA efficiently and specifically silenced (more than 70%) p53 expression in MC3T3-E1 osteoblasts (Fig. 6A). In control siRNA transfected osteoblasts, treatment with BBP increased Bax and caspase 9 while decreased cyclin D3, as above observed in non-transfected osteoblasts. Conversely, treatment with BBP on osteoblasts p53 silenced, in addition to decrease Bax and cleaved caspase 9, induced an increase of cyclin D3

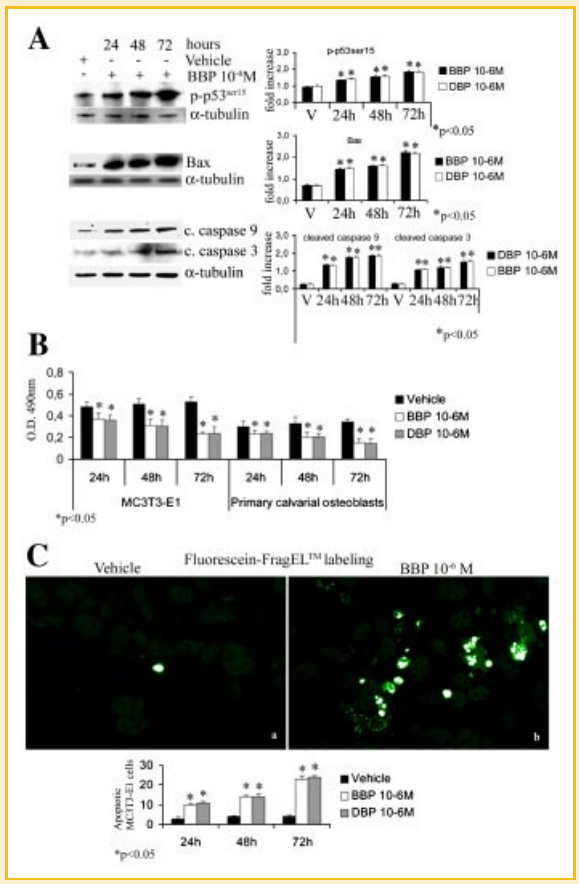

Fig. 5. A: Daily BBP treatment in MC3T3-E1 osteoblasts. phospho-p53 (ser-15), Bax, cleaved caspase 9 and cleaved caspase 3 levels were analyzed by Western blotting as described in Materials and Methods Section. Cells were serum deprived for 24 h and treated daily with BBP (10^{-6} M), DBP (10^{-6} M), or vehicle from 24 up to 72 h. Proteins (5 μg) from each sample were subjected to SDS–PAGE, transferred to PVDF membrane and probed with rabbit anti-phospho-p53 (ser-15), rabbit anti-Bax, rabbit anti-cleaved caspase 9 and rabbit anti-cleaved caspase 3 antibodies; then, filters were stripped and re-probed with mouse anti-α-tubulin antibody to show equal amount of loading. B: Effect of BBP and DBP daily treatment on the metabolic activity of viable MC3T3-E1 osteoblasts and COBs. Cells were serum deprived for 24 h and daily treated with BBP (10^{-6} M), DBP (10^{-6} M), or vehicle for 24, 48, and 72 h. Values are mean ± SEM for three different experiments. To note the time-dependent decrease of osteoblasts viability after phthalates treatment; $^{*}P < 0.05$. C: Effect of daily BBP and DBP treatment on DNA fragmentation. Cells were serum deprived for 24 h and treated with BBP (10^{-6} M), DBP (10^{-6} M), or vehicle for 24, 48, and 72 h. Representative photomicrographs of Fluorescein-FragEL-positive osteoblasts that increased after 72 h of BBP treatment (b) respect to vehicle treated osteoblasts (a). The quantitative analyses were performed as previously described in Materials and Methods Section. Values were referred as means ± SD and statistically analyzed with *t*-test operating on PC computer; $^{*}P < 0.05$.

(Fig. 6B). Similar results were obtained with DBP treatment (data not shown).

Data from MTS assay indicated that BBP and DBP cause a decrease of viable osteoblasts transfected with control siRNA, as above observed in non-transfected cells; instead, BBP and DBP increased p53 knockdown osteoblasts viability (Fig. 6C).

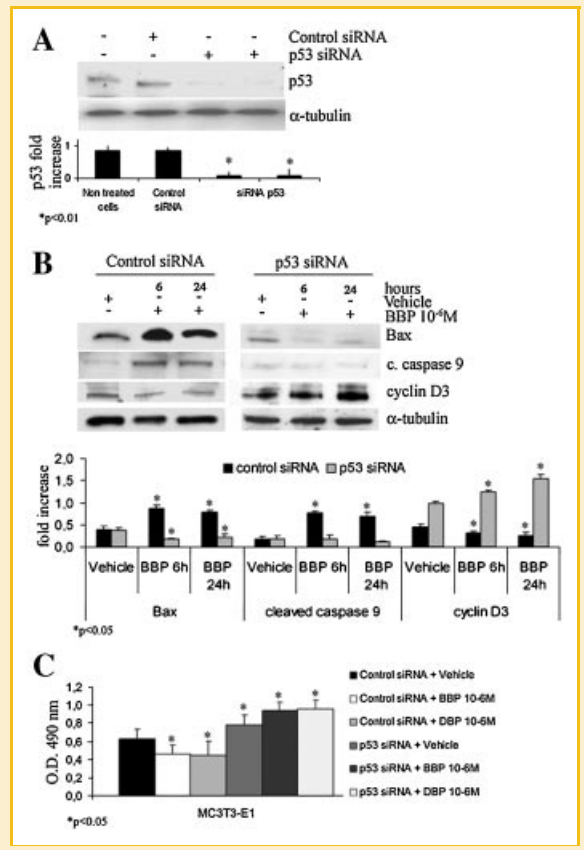

Fig. 6. A: Depletion of endogenous p53 by RNAi in MC3T3-E1 osteoblasts. Cells were transfected with p53 siRNA or control siRNA and the level of p53 protein was analyzed by Western blotting as described in Materials and Methods Section. Proteins (5 μg) from each sample were subjected to SDS–PAGE, transferred to PVDF membrane and probed with rabbit anti-p53 antibody; then, filters were stripped and re-probed with monoclonal anti-α-tubulin antibody to show equal amount of loading. B: Effects of BBP on Bax, cleaved caspase 9 and cyclin D3 in MC3T3-E1 osteoblats transfected with p53 siRNA. After transfection, as above described, cells were serum deprived for 24 h and treated with BBP (10^{-6} M) or vehicle for 6 and 24 h. Proteins (5 μg) from each sample were subjected to SDS–PAGE, transferred to PVDF membrane and probed with rabbit anti-Bax, rabbit anti-cleaved caspase 9 and mouse anti-cyclin D3 antibodies; then, filters were stripped and reprobed with monoclonal anti-α-tubulin antibody to show equal amount of loading. C: Effects of BBP and DBP on the metabolic activity of viable MC3T3-E1 osteoblasts transfected with p53 siRNA. After transfection, as above described, cells were serum deprived for 24 h and treated with BBP (10^{-6} M), DBP (10^{-6} M), or vehicle. Values are mean ± SEM for three different experiments. Note that BBP statistically increased cell viability in p53 siRNA transfected osteoblasts; $^{*}P < 0.05$.

EFFECTS OF PHTHALATES ON p53 AND PHOSPHO-p53 IN PY1A RAT OSTEOBLAST

We previously demonstrated that, in Py1a rat osteoblasts, phthalates did not modify Bcl2/Bax ratio, while increased cyclin D3 and cell proliferation; conversely, actual data showed that only p53 silenced mouse osteoblasts gave a response to phthalates similar to that observed in Py1a rat osteoblasts. Hence the effects of BBP on p53 and phospho-p53 in Py1a cells were investigated.

Surprisingly, treatment with BBP for 6 and 24 h did not substantially modify p53, phospho-p53 (ser-15), and phospho-p53

(ser-20) levels (Fig. 7A). Pooled data from three different experiments better clarified that BBP do not modify the above proteins (Fig. 7B).

Data from CLSM demonstrated that treatment with BBP increase phospho-p53 (ser-15) labeling in MC3T3-E1 mouse osteoblasts. Conversely, the effector did not modify phospho-p53 (ser-15) staining in Py1a rat osteoblasts (Fig. 7C). Confocal microscopy data were also supported by immunogold labeling carried out on ultrathin sections where a basic occurrence of phospho-p53 (ser-15) was observed in vehicle Py1a and MC3T3-E1 cells. After 6 h of BBP treatment Py1a cells labeling was unchanged, while MC3T3-E1 cells nuclear labeling was increased (Fig. 7D). In order to quantify phospho-p53 (ser-15) labeling, a statistical analysis was performed. Gold particle count showed mean labeling density of 23.333 ± 2 μm^2 in vehicle treated MC3T3-E1 cells and mean labeling density of 38.667 ± 2.5 μm^2 after BBP treatment; conversely mean labeling densities of 7.667 ± 0.5 μm^2 and 8.333 ± 0.8 μm^2 were observed in vehicle and BBP treated Py1a osteoblasts, respectively (Fig. 7E). Control experiments produced no appreciable staining both at CLSM and IEM level (data not shown).

DISCUSSION

It was previously demonstrated that BBP and DBP, in addition to act in a dose- and a time-dependent manner, caused cell cycle

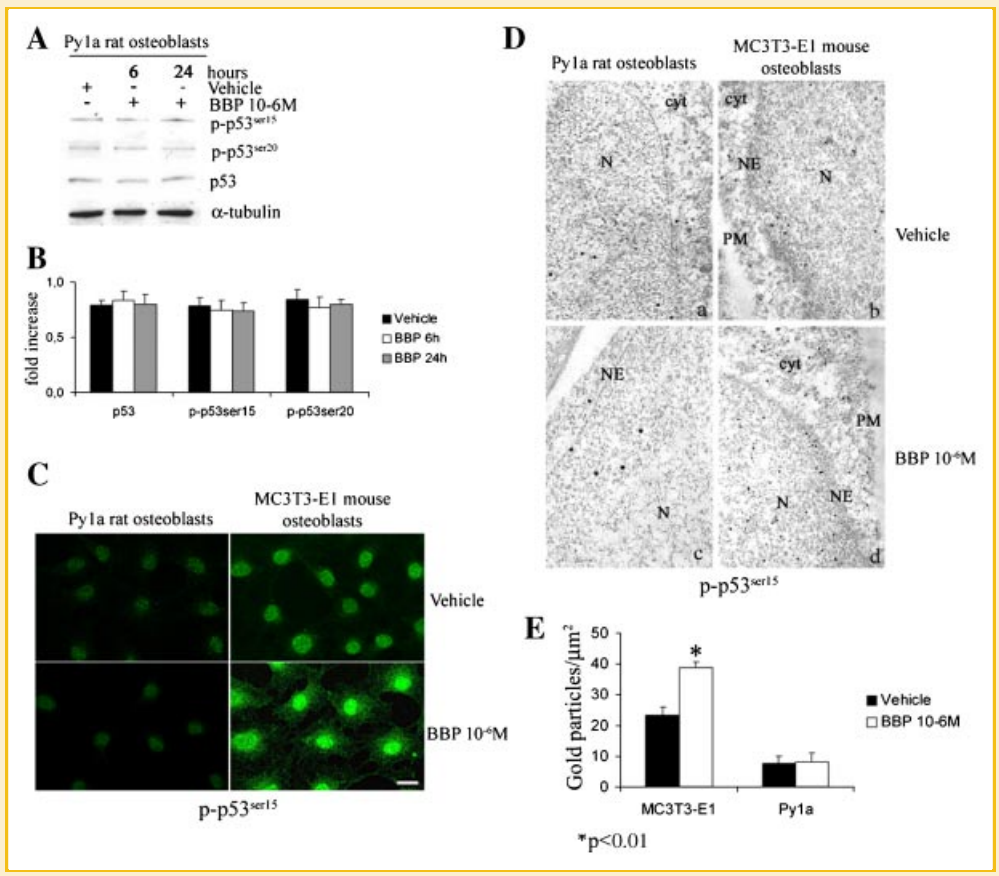

Fig. 7. A: Effect of BBP on p53, phospho-p53 (ser-15), and phospho-p53 (ser-20) in Py1a rat osteoblasts. p53, phospho-p53 (ser-15), and (ser-20) levels were analyzed by Western blotting as described in Materials and Methods Section. Cells were serum deprived for 24 h and treated with BBP (10^{-6} M) or vehicle for additional 6 and 24 h. Proteins (5 μg) from each sample were subjected to SDS–PAGE, transferred to PVDF membrane and probed with rabbit anti-p53, rabbit anti-phospho-p53 (ser-15), or with rabbit anti-phospho-p53 (ser-20) antibodies; then, filters were stripped and reprobed with monoclonal anti-α-tubulin antibody to show equal amount of loading. Note that BBP treatment did not statistically modified the levels of the p53 and the phospho-p53 examined. B: Statistical analysis from a pool of three different experiments showing the effects of BBP on p53, phospho-p53 (ser-15), and phospho-p53 (ser-20) in Py1a rat osteoblasts. Values were referred as means $\pm$ SD and statistically analyzed with *t*-test operating on PC computer. Note that treatment with BBP did not significantly modify the examined proteins, compared to vehicle treated cells; $^{*}P < 0.05$. C: CLSM—Effect of BBP on phospho-p53 (ser-15) labeling in Py1a and MC3T3-E1 osteoblasts. Cells were serum deprived and treated with BBP (10^{-6} M) for 6 h. Localization of phospho-p53 (ser-15) was analyzed by CLSM using the rabbit anti-phospho-p53 (ser-15) antibody (green: FITC staining). Bar, 50 μm. D: IEM –Effect of BBP on phospho-p53 (ser-15) distribution in Py1a and MC3T3-E1 osteoblasts. Immunogold labeling of phospho-p53 (ser-15) analyzed by transmission electron microscopy. IEM from vehicle treated cells better depicted the above showed basal labeling for phospho-p53 (ser-15) in Py1a rat osteoblasts (a) and in MC3T3-E1 mouse cells (c). Note a nuclear increase of labeling particularly evident after 6 h of BBP (10^{-6} M) treatment only in MC3T3-E1 osteoblasts (d). PM, plasma membrane; cyt, cytoplasm; NE, nuclear envelope; N, nucleus. a, ×26,200; b, ×29,400; c, ×21,400; d, ×16,500. E: The IEM images of 6 h BBP treated cells and vehicle were scanned by the computer. The labeling density was estimated on cell surface areas of 16 samples in each experimental group. Values were referred as means $\pm$ SD and statistically analyzed with *t*-test operating on PC computer. Note the significant increase in 6 h BBP treated cells compared to vehicle only in mouse osteoblasts; $^{*}P < 0.01$.

progression and proliferation in Py1a rat osteoblasts [Menghi et al., 2001; Agas et al., 2007]. In the present report we focused our attention on BBP (10^{-6} M) and DBP (10^{-6} M) effects in MC3T3-E1 osteoblasts and COBs.

First, we demonstrated that both BBP or DBP provoke a statistically significant increase of DNA damage and a related phosphorylation of ATM (ser-1981) was also observed. It is known that after DNA damage, p53 protein accumulates rapidly through a post-trascriptional mechanism and it is also activated as a transcriptional factor, which then leads to growth arrest or apoptosis [Levine, 1997]. Indeed, a significant increase of both p53 and phospho-p53 (ser-15 and ser-20) was found in MC3T3-E1 BBP treated osteoblasts.

In the light of the above data, we determined the effects of phthalate administration on critical apoptosis regulators and we found an increase of Bax levels in particular on the mitochondrial fraction. An increase of cytochrome *c* on the mitochondrial fraction at 2 h and on the cytoplasmic fraction at 24 h of BBP administration was observed. Moreover, an increase of Apaf-1 as well as cleaved caspases 9 and 3 was evidenced. Since it has been demonstrated that the release of mitochondrial cytochrome *c* into the cytoplasm is thought to be a critical step in the activation and maturation of a multimeric complex, the apoptosome, comprising cytochrome *c*, Apaf-1 and caspase 9 [Liu et al., 1996; Li et al., 1997; Vaux 1997; Zou et al., 1997], in our experiments the increase of cytochrome *c* and Apaf-1 were likely due to the stabilization of the apoptosome and the initiation of the apoptotic cascade.

It has been shown that the proto-oncogene c-myc is required for entry into cell cycle progression by cyclin D [Berns et al., 2000]. Of the signal transduction pathways, cyclin dependent kinases (Cdks) are the key downstream regulators of c-myc and the activity of Cdks is regulated by cyclin dependent kinase inhibitors (CKIs) [Sherr and Roberts, 1999]. In addition, c-myc stimulates the expression of cyclin A, D1, D3, E, Cdk2, Cdk4 [Born et al., 1994; Kim et al., 1994; Beier et al., 2000] and represses the expression of p21 and p27 [Zajac-Kaye, 2001]. Accordingly, we evaluated cell cycle regulators like c-myc, cyclin D and CDK4. Treatment with BBP or DBP decreased c-myc, cyclin D3 and CDK4 at 2, 4, and 6 h. Indeed, it has been well documented that the cyclin D-Cdk4/6 complex specifically phosphorylates Rb protein at Ser-780 [Zarkowska and Mittnacht, 1997; Malumbres and Barbacid, 2001]. Accordingly, a reduction in ser-780 Rb phosphorylation levels in parallel with a decrease in Cdk4 protein levels was observed; conversely, an increase of apoptotic markers above detailed was found. To gain further insights into the effects of phthalates on mouse osteoblast apoptosis, the MTS assay was performed; findings indicated that phthalates cause a reduced cell viability after 24 h of treatment. We also investigated the effects of BBP on the MC3T3-E1 distribution through the cell cycle by flow cytometry and found that osteoblasts are overall at G0/G1 phase after 24 h of treatment. It should be noted that the cell cycle arrest is concomitant with the trend of Fluorescein FragEL™ assay.

BBP and DBP daily administration amplified all the apoptotic markers suggesting that phthalates could exert cumulative effects. The complex of present data indicated that the exposure of mouse osteoblasts to BBP or DBP causes bone perturbance; indeed, induction of DNA damage and activation of apoptotic pathways were observed by multiple approaches. The chronic exposure to phthalates at low concentrations could probably affect new bone formation and matrix deposition with clinical implications on bone homeostasis and mineral density.

Additional information about p53, as the most valid candidate responsible of apoptosis induction, originated from experiments on p53-silenced osteoblasts exposed to BBP and DBP. Results demonstrated that, in p53-silenced cells, phthalates caused cell proliferation consistent with increased c-myc and cell cycle regulator levels. It has been reported that the differential expression of the cyclins and CDKs known to be either directly regulated by p53 or downstream events of p53 expression and the expression of genes regulated by p53 (directly or indirectly) would not be the same in wild-type and p53 null animals [Hirai and Sherr, 1996; Morris et al., 2008]. Accordingly our findings showed that in p53 knockdown mouse osteoblasts, phthalates increase proliferation by involvement of cyclins D.

In a previous research we demonstrated that both BBP and DBP induced increase of cyclin D3 levels as well as cell viability in Py1a rat osteoblasts; however, the not significant change of Bcl-2/Bax ratio indicated that the increase of cell viability, induced by the effectors, could be due to cell proliferation [Agas et al., 2007]. To explain the differential effects of phthalates in mouse and rat osteoblasts, we considered interesting to evaluate the expression of phospho-p53 also in Py1a rat osteoblasts treated with BBP and we found that phospho-p53 levels were not substantially modified. The increase of p53 nuclear labeling in mouse osteoblasts suggests that these proteins could activate the expression of the stress responsive genes resulting in apoptosis as demonstrated in different organ tissues [Cotton and Spandau, 1997; Middeler et al., 1997; Reinke and Lozano, 1997]. It is also possible to hypothesize that, in Py1a cells, BBP treatment evoked a proliferative response, as above demonstrated in p53 silenced mouse osteoblasts, rather than p53 activation

An important question is to elucidate the functional meaning of increased p53 that was only found in treated mouse osteoblasts. This is a prerequisite for understanding the mechanism by which phthalates, as EDs, regulate the fate of the cells.

ACKNOWLEDGMENTS

The authors would like to thank Mrs. S. Cammertoni and Mr. S. Riccioni for the technical assistance.

REFERENCES

Agas D, Sabbieti MG, Capacchietti M, Materazzi S, Menghi G, Materazzi G, Hurley MM, Marchetti L. 2007. Benzyl butyl phthalate influences actin distribution and cell proliferation in rat Py1a osteoblasts. J Cell Biochem 101:543–551.

Attardi LD, Reczek EE, Cosmas C, Demicco EG, McCurrach ME, Lowe SW, Jacks T. 2000. PERP, an apoptosis-associated target of p53, is a novel member of the PMP-22/gas3 family. Genes Dev 14:704–718.

Banin S, Moyal L, Shieh S, Taya Y, Anderson CW, Chessa L, Smorodinsky NI, Prives C, Reiss Y, Shiloh Y, Ziv Y. 1998. Enhanced phosphorylation of p53 by ATM in response to DNA damage. Science 281:1674–1677.

Beier R, Bürgin A, Kiermaier A, Fero M, Karsunky H, Saffrich R, Möröy T, Ansorge W, Roberts J, Eilers M. 2000. Induction of cyclin E-cdk2 kinase

activity, E2F-dependent transcription and cell growth by Myc are genetically separable events. EMBO J 19:5813–5823.

Berns K, Hijmans EM, Koh E, Daley GQ, Bernards R. 2000. A genetic screen to identify genes that rescue the slow growth phenotype of c-myc null fibroblasts. Oncogene 19:3330–3334.

Born TL, Frost JA, Schönthal A, Prendergast GC, Feramisco JR. 1994. c-Myc cooperates with activated Ras to induce the cdc2 promoter. Mol Cell Biol 14:5710–5718.

Bunz F, Dutriaux A, Lengauer C, Waldman T, Zhou S, Brown JP, Sedivy JM, Kinzler KW, Vogelstein B. 1998. Requirement for p53 and p21 to sustain G2 arrest after DNA damage. Science 282:1497–1501.

Cotton J, Spandau DF. 1997. Ultraviolet B-radiation dose influences the induction of apoptosis and p53 in human keratinocytes. Radiat Res 147:148–155.

Dewey WC, Ling CC, Meyn RE. 1995. Radiation-induced apoptosis: Relevance to radiotherapy. Int J Radiat Oncol Biol Phys 33:781–796.

Ema M, Itami T, Kawasaki H. 1993. Teratogenic phase specificity of butyl benzyl phthalate in rats. Toxicology 79:11–19.

Fei P, El-Deiry WS. 2003. P53 and radiation responses. Oncogene 22:5774–5783.

Group EF, Jr. 1986. Environmental fate and aquatic toxicology studies on phthalate esters. Environ Health Perspect 65:337–340.

Guillette LJ, Jr., Guillette EA. 1996. Environmental contaminants and reproductive abnormalities in wildlife: Implications for public health? Toxicol Ind Health 12:537–550.

Harris CA, Henttu P, Parker MG, Sumpter JP. 1997. The estrogenic activity of phthalate esters. In Vitro Environ Health Perspect 105:802–811.

Hecht R, Connelly M, Marchetti L, Ball WD, Hand AR. 2000. Cell death during development of intercalated ducts in the rat submandibular gland. Anat Rec 258:349–358.

Hirai H, Sherr CJ. 1996. Interaction of D-type cyclins with a novel myb-like transcription factor, DMP1. Mol Cell Biol 16:6457–6467.

Jobling S, Reynolds T, White R, Parker MG, Sumpter JP. 1995. A variety of environmentally persistent chemicals, including some phthalate plasticizers, are weakly estrogenic. Environ Health Perspect 103:582–587.

Kim YH, Buchholz MA, Chrest FJ, Nordin AA. 1994. Up-regulation of c-myc induces the gene expression of the murine homologues of p34cdc2 and cyclin-dependent kinase-2 in T lymphocytes. J Immunol 152:4328–4335.

Levine AJ. 1997. p53, the cellular gatekeeper for growth and division. Cell 88:323–331.

Li P, Nijhawan D, Budihardjo I, Srinivasula SM, Ahmad M, Alnemri ES, Wang X. 1997. Cytochrome c and dATP-dependent formation of Apaf-1/caspase-9 complex initiates an apoptotic protease cascade. Cell 91:479–489.

Liu X, Kim CN, Yang J, Jemmerson R, Wang X. 1996. Induction of apoptotic program in cell-free extracts: Requirement for dATP and cytochrome c. Cell 86:147–157.

Longnecker MP, Rogan WJ, Lucier G. 1997. The human health effects of DDT (dichlorodiphenyltrichloroethane) and PCBS (polychlorinated biphenyls) and an overview of organochlorines in public health. Annu Rev Public Health 18:211–244.

Malumbres M, Barbacid M. 2001. To cycle or not to cycle: A critical decision in cancer. Nat Rev Cancer 1:222–231.

Marchetti L, Sabbieti MG, Menghi M, Materazzi S, Hurley MM, Menghi G. 2002. Effects of phthalate esters on actin cytoskeleton of Py1a rat osteoblasts. Histol Histopathol 17:1061–1066.

Marchetti L, Sabbieti MG, Agas D, Menghi M, Materazzi G, Menghi G, Hurley MM. 2006. PGF2α increases FGF-2 and FGFR2 trafficking in Py1a rat osteoblasts via clathrin independent and importin β dependent pathway. J Cell Biochem 97:1379–1392.

Mayer FL, Stalling DL, Johnson JL. 1972. Phthalate esters as environmental contaminants. Nature 238:411–413.

Menghi G, Sabbieti MG, Marchetti L, Menghi M, Materazzi S, Hurley MM. 2001. Phthalate esters influence FGF-2 translocation in Py1a rat osteoblasts. Eur J Morphol 39:155–162.

Middeler G, Zerf K, Jenovai S, Thulig A, Tschodrich-Rotter M, Kubitscheck U, Peters R. 1997. The tumor suppressor p53 is subject to both nuclear import and export, and both are fast, energy-dependent and lectininhibited. Oncogene 14:1407–1417.

Montero A, Okada Y, Tomita M, Ito M, Tsurukami H, Nakamura T, Doetschman T, Coffin JD, Hurley MM. 2000. Disruption of the fibroblast growth factor-2 gene results in decreased bone mass and bone formation. J Clin Invest 105:1085–1093.

Morgan SE, Kastan MB. 1997. p53 and ATM: Cell cycle, cell death, and cancer. Adv Cancer Res 71:1–25.

Morris SM, Akerman GS, Desai VG, Tsai C, Tolleson WH, Melchior WB, Lin C-J, Fuscoe JC, Casciano DA, Chen JJ. 2008. Effect of p53 genotype on gene expression profiles in murine liver. Mut Res 640:54–73.

Offer H, Erez N, Zurer I, Tang X, Milyavsky M, Goldfinger N, Rotter V. 2002. The onset of p53-dependent DNA repair or apoptosis is determined by the level of accumulated damaged DNA. Carcinogenesis 23:1025–1032.

Ohki R, Nemoto J, Murasawa H, Oda E, Inazawa J, Tanaka N, Taniguchi T. 2000. Reprimo, a new candidate mediator of the p53-mediated cell cycle arrest at the G2 phase. J Biol Chem 275:22627–22630.

Parfitt AM. 1987. Bone remodelling and bone loss-understanding the pathophysiology of osteoporosis. Clin Obstet Gynecol 30:789–811.

Pawley J. 1995. Fundamental limits in confocal microscopy. In: Pawley J, editor. Handbook of biological confocal microscopy. 2nd edition. New York and London: Plenum Press. pp. 19–37.

Quarles LD, Yohay DA, Lever LW, Caton R, Wenstrup RJ. 1992. Distinct proliferative and differentiated stages of murine MC3T3-E1 cells in culture: An in vitro model of osteoblast development. J Bone Miner Res 7:683–692.

Reinke V, Lozano G. 1997. Differential activation of p53 targets in cells treated with ultraviolet radiation that undergo both apoptosis and growth arrest. Radiat Res 148:115–122.

Rodan GA. 1992. Introduction to bone biology. Bone 13:S3–S6.

Ross GM. 1999. Induction of cell death by radiotherapy. Endocr Relat Cancer 6:41–44.

Sabbieti MG, Marchetti L, Curini R, Menghi G, Roda A, Russo MV, Nugnes C, Materazzi S. 2000. Evidence of butyl benzyl phtalate induced modifications in a model system developed in vitro. Analusis 28:843–846.

Safe SH. 1998. Interactions between hormones and chemicals in breast cancer. Annu Rev Pharmacol Toxicol 38:121–158.

Savitsky KA, Bar-Shira S, Gilad G, Rotman Y, Ziv L, Vanagaite DA, Tagle S, Smith T, Uziel S, Ashkenazi M, Pecker I, Frydman M, Harnik R, Patanjali SR, Simmons A, Clines GA, Sartiel A, Gatti RA, Chessa L, Sanal O, Lavin MF, Jaspers NG, Taylor AM, Arlett CF, Miki T, Weissman SM, Lovett M, Collins FS, Shiloh Y. 1995. A single ataxia telangiectasia gene with a product similar to PI-3 kinase. Science 268:1749–1753.

Sharman M, Read WA, Castle L, Gilbert J. 1994. Levels of di-(2-ethylhexyl)phthalate and total phthalate esters in milk, cream, butter and cheese. Food Addit Contam 11:375–385.

Sherr CJ, Roberts JM. 1999. CDK inhibitors: Positive and negative regulators of G1-phase progression. Genes Dev 13:1501–1512.

Shotton N. 1989. Confocal scanning optical microscopy and its applications for biological specimens. J Cell Science 94:175–206.

Siliciano JD, Canman CE, Taya Y, Sakaguchi K, Appella E, Kastan MB. 1997. DNA damage induces phosphorylation of the amino terminus of p53. Genes Dev 11:3471–3481.

Stein GS, Lian JB. 1993. Molecular mechanisms mediating proliferation/differentiation interrelationships during progressive development of the osteoblast phenotype. Endocr Rev 14:424–442.

Tanaka H, Arakawa H, Yamaguchi T, Shiraishi K, Fukuda S, Matsui K, Takei Y, Nakamura Y. 2000. A ribonucleotide reductase gene involved in a p53-dependent cell-cycle checkpoint for DNA damage. Nature 404: 42–49.

Vaux DL. 1997. CED-4 the third horseman of apoptosis. Cell 90:389–390.

Zajac-Kaye M. 2001. Myc oncogene: A key component in cell cycle regulation and its implication for lung cancer. Lung Cancer 2:S43–S46.

Zarkowska T, Mittnacht S. 1997. Differential phosphorylation of the retinoblastoma protein by G1/S cyclin-dependent kinases. J Biol Chem 272:12738–12746.

Zou H, Henzel WJ, Liu X, Lutschg A, Wang X. 1997. Apaf-1, a human protein homologous to C. elegans CED-4, participates in cytochrome c-dependent activation of caspase-3. Cell 90:405–413.